Cumhuriyet Sci. J., 43(4) (2022) 760-768
DOI: https://doi.org/10.17776/csj.1188709

Cumhuriyet Science Journal

| csj.cumhuriyet.edu.tr | Founded: 2002 ISSN: 2587-2680 e-ISSN: 2587-246X Publisher: Sivas Cumhuriyet University

Searching for New Supernova Remnant Candidates from the VTSS Survey

Elif Beklen [1,a,*]

[1] *Department of Physics, Faculty of Arts and Sciences, Süleyman Demirel University, Isparta, Türkiye*
**Corresponding author*

Research Article

History
Received: 13/10/2022
Accepted: 07/12/2022

ABSTRACT

The Virginia Tech Spectral Line Survey (VTSS) Galactic Plane Hydrogen-Alpha Survey has the strong ability to search and discover many different types of objects that cannot be identified clearly on red plates and by other Multi-Wavelength Sky Surveys. Here we make a visual search from the VTSS fields with the supportive surveys of Southern Hydrogen-Alpha Sky Survey Atlas (SHASSA) and MDW Hydrogen-Alpha Sky Survey (MDWS) fields, in the Galactic latitude of |b| between -17 ° and 7 ° for several new optical emission nebulae. Seven candidates were chosen as most likely supernova remnant candidates by their physical shapes and the three of all having [SII]/Hα ratio larger than 0.4, found with T100 photometric observations, are considered to be supernova remnant candidates. Comprehensive optical imaging and spectroscopic observations with multi-wavelength observations will help us to identify the types of all these galactic candidates, more precisely.

Keywords: Surveys, ISM: supernova remnants, Optical

[a] *elifbeklen@gmail.com* *https://orcid.org/0000-0002-4807-2180*

Introduction

Supernova remnants (SNRs) are important objects to understand the evolution of the interstellar medium (ISM) and galaxies. To better understand our galaxy, all of the studies including detecting individual SNRs with an accurate number of Galactic total SNRs become important. There is an apparent divergence between the number of observed and expected Galactic SNRs based on supernovae rates. Currently, there are nearly 300 Galactic SNRs with the most majority discovered through radio observations and some of in X-ray observations [1-4].

Even though less than half of Galactic SNRs show any appreciable optical emission, optical studies of SNRs are useful and become important for dynamical properties in all remnants, and for the kinematics of ejecta in the youngest remnants. For some remnants, a remnant's optical emission can also help to define its overall size and morphology. This is especially true for some radio weak emission or radio-quiet SNRs exhibiting significant optical emission [5-11]. About 40% of the detected Galactic SNRs show associated X-ray emission with a smaller percentage (~30%) showing some coincident optical emission [12]. Although discoveries of Galactic remnants in the optical are less according to others, several [13-15] have recently been made through deep Hα surveys such as the Hα emission Virginia Tech Spectral Line Survey (VTSS) of the Galactic Plane [16, 17] (e.g. the optical discovery of G159.6+7.3 [14]), the Southern Hydrogen-Alpha Sky Survey Atlas (SHASSA) [18], MDW Hydrogen-Alpha Survey (MDWS) and the Isaac Newton Telescope Photometric Hydrogen Survey [19, 20].

The imaging filters flux ratio of [SII(6717, 6731)]/H(6563) ≥ 0.4 (firstly proposed by Mathewson and Clarke 1973 [21]) has been using as a well-known and successful observational criterion to differentiate SNRs from other type of optical emission nebulae in both Galactic and extragalactic searches [11, 22-26]. Mainly, the general idea is expecting SNRs to give higher values of [SII] than HII regions since behind the shock front the collisionally excited gives strong [SII] emission, while in HII regions sulphur is mostly in the form of S^{++}.

The goal of this work is to discover new supernova remnant candidates through Hα survey by visual selection of the size or shapes similar to the detected supernova remnants appearance observed through the same survey. The emission fields can also include HII-regions, all of which can be the same in appearance. So, we report a search for large and mid-size possible Galactic SNR candidates through its Hα optical emission by using archival VTSS Survey images with the help of SHASSA and MDWS Surveys, and the latest SNR and HII-region catalogs.

Surveys

The VTSS (http://www1.phys.vt.edu/~halpha/#Images) covers a wide region around the northern Galactic plane (15 ° < l < 230 °, |b| <= 30 °), north of δ > -15 °, and gain importance in the study of Galactic supernova remnants, HII regions, and many different Hα emission sources. 107 fields have been released on the VTSS Web site. The VTSS survey used a fast short-focus lense of f/1.2 camera lens with a 58-mm focal length, together with a 512 x 512 CCD array that projected to 96 arcsec/pixel on the sky. Its Hα filter had a FWHM of 17.5 **Å**, transmitting mainly the Hα line.

Other Hα imaging surveys, SHASSA and MDWS are used to search the emission structures that the zone covered by the VTSS survey images. SHASSA is an imaging survey covering 21000deg2 of the southern and equatorial sky undertaken with the aim of detecting Hα emission from the ionized interstellar medium. The survey consists of 2168 images covering 542 fields south of +16° declination, between Galactic longitudes of 195° and 45° at the mid-plane (GMR01). The SHASSA survey used a fast short-focus lense of f/1.6 camera lens with a focal length of 52 mm, together with 1024 x 1024 CCD array that projected to 48 arcsec/pixel on the sky. Its Hα filter had a FWHM of 32 **Å** ([27], [28]). For both VTSS and SHASSA fields, the continuum-subtracted (generated by subtracting each continuum image from the corresponding Hα image) and then smoothed images (for SHASSA survey; saved as SHASSA_CC) are used. Even though to have lower angular resolution both surveys are very deep and are a useful tools to search for any extended large high-latitude nebulae emission. These surveys become a key tool for searching possible SNRs that may have been missed in previous searches.

Another survey used during this search is the MDWS (https://www.mdwskysurvey.org) with its wide field-of-view (FoV) of approximately 3°.5 × 3°.5 with a pixel size of 3".17 and relatively low-resolution images, it reveals deeper, more complex and quite extensive optical filaments and structures visible in higher resolution images. This survey consists of a 130 mm telescope at the New Mexico Skies Observatory, with an FLI ProLine 16803 CCD and a 3 nm filter centered on Hα [11]. There are 2771 fields under the MDWS website and the exposure times used for the observation of each field was 12x1200 s.

Observations and Data Analysis

The optical imaging observations for some of these emission fields were performed with the

1-meter Turkish Telescope T100, located in TÜBITAK National Observatory of Turkey's (TUG) (https://tug.tubitak.gov.tr/tr/teleskoplar/t100-odak-duzlemi-aletleri). We get high-quality photometry by using a cryo-cooler SI 1100 CCD with 4096 x 4096 pixels, with an effective field of view (FoV) of 21'.5 x 21'.5. We used narrow passband interference filters (FWHM = 80 **Å**) (λ = 6563 **Å**) Hα, (FWHM = 54 **Å**) (λ = 6728 **Å**) [SII] and Bessel R filter as continuum filter to remove starlight background from the narrow passband filters images of these regions. The exposure times were 900 s for each narrow band filter with 2 x 200 s for the continuum band filter.

T100 images were reduced by using the reduction photometry pipelines in astropy. Both the bias and flat-field frames for each image were also obtained and during the reduction, the cosmic hits were also removed by using a median-averaged process during the bias-subtraction and flat-fielding of the images. During the observations, we use the Digitized Sky Survey (DSS1 or DSS2) (The STScI Digitized Sky Survey; https://archive.stsci.edu/cgi-bin/dss_form) images as the confirmation of the selected positions of the approximate central coordinates of each candidate.

Methods, Results and Discussion

We will discuss our work done by a visual search conducted of all VTSS fields plus the surveys of SHASSA and MDWS fields that are currently available online. All of the surveys contain wide-field and small-scale Hα emission structures, and among these structures, a significant number of supernova remnants will be discovered. These Galactic Hα Surveys have high promise to increase our knowledge of optical supernova remnants and their physical properties. In this work, the VTSS Survey images were primarily scanned and visual search was done individually on each field. The selection criteria on the appropriate field images were choosing the field either consisting of previously detected supernova remnants and HII-regions or fully undetected emission structures.

The Orion 08 first and second regions, respectively Ori08(A) and Ori08(B) (see the left and right side of the first row in Figure 1, and for the coordinates see Table 1), are the two selected emission candidates under the Ori08 field in the VTSS Survey. These regions are also observed with the continuum-subtracted SHASSA survey and both survey images are confirming each other. These regions are scanned with their close environments by using the WISE Catalog of Galactic HII-Regions (http://astro.phys.wvu.edu/wise/) (version 2.4, [29]) and it was seen that the wide-field Orion region does not include any detected HII regions. Also, the wide-field Orion region was also scanned according to the Green 2019 catalog to explore any detected and known supernova remnants. As a result, there are no identified SNRs in this region. Another SNR and HII-free region located in the Monoceros-Mon07 field in the archive VTSS survey is named Mon07(A) (the image on the right side of the second row in Figure 1). The emission is in partial shape, maybe a part of the composite structure detectable explicitly in another band. This structure can also be observed with the SHASSA survey, and both VTSS and SHASSA images are matching well with each other.

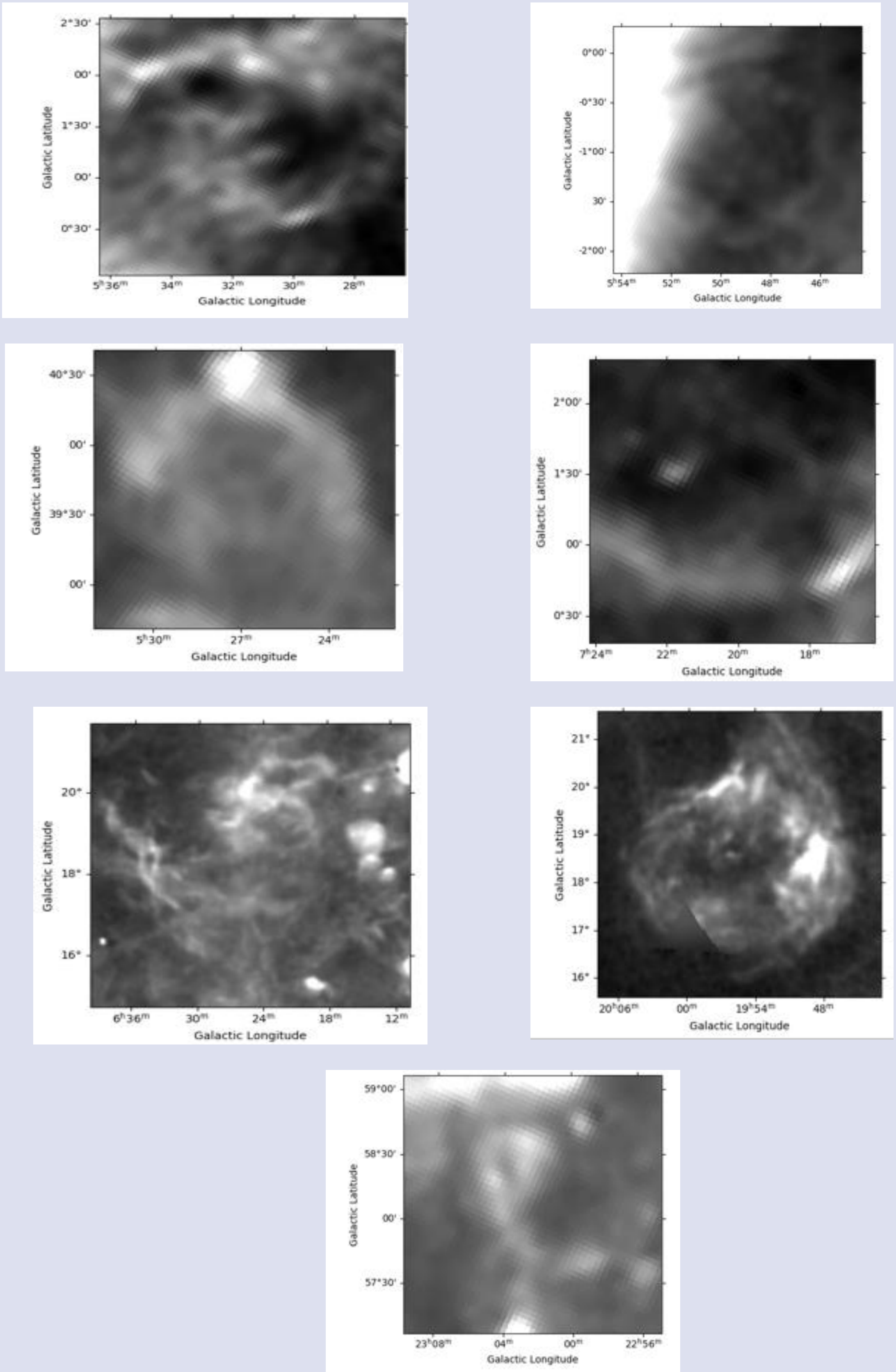

Figure 1. Hα image of optical emission nebulae from the VTSS Survey of the Galactic Plane. North is up, east to the left with (J2000.0) coordinates and the occupied area of the regions are shown in Table 1.

Table 1. Central coordinates of the selected emission nebulae fields with their surrounding areas. The last column shows the used surveys for confirming the same structural regions. In each survey, the structures can be visually identified with the same dimensions, clearly

Region Name	R.A. (J2000.0)	Dec. (J2000.0)	Candidate Dimension (Degree °)	Used Surveys
Ori08(A)	05:31:37	+01:24:56	2.5	VTSS, SHASSA, MDWS
Ori08(B)	05:48:58	-01:03:06	2.5	VTSS, SHASSA, MDWS
Aur05(A)	05:26:57	+39:38:02	1.0	VTSS, MDWS
Mon07(B)	06:27:19	+18:29:10	2.5	MDWS
Mon07(A)	07:20:10	+01:18:30	1.0	VTSS, SHASSA
Sge01(A)	19:55:23	+18:37:09	2.5	VTSS
Cep00(A)	23:02:19	+58:07:32	0.8	VTSS

The other four candidates are all located in crowded regions in a sense of previously detected SNRs and HII-regions with well-known locations and sizes. The Mon07(B) (the left image on the third row in Figure 1 with a radius of approximately 2.5°) is visually first noticed in the MDW survey since it is not clearly visible in the wide-field Mon07 VTSS survey image. There are no detected SNRs in the wide-field region with a size of approximately 7° whereas some labeled HII-regions are taken from WISE-HII region catalog (red circles in the right side of the first row in Figure 2; the candidate is shown with clay circle).

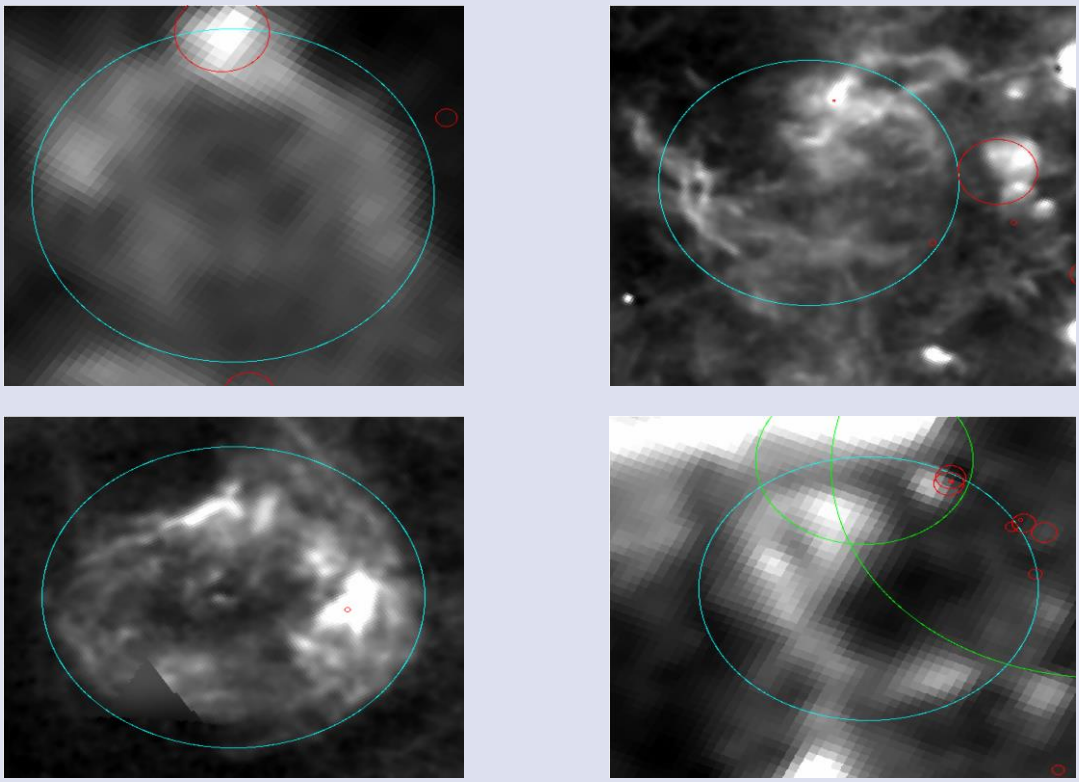

Figure 2. Hα image of optical emission nebulae from the VTSS Survey of the Galactic Plane. North is up, east to the left with (J2000.0) coordinates and the occupied area of the regions are shown in Table 1.

For the Auriga-Aur05 field under the sky survey, in the emission region named Aur05(A) (the left image on the second row in Figure 1) there is one large HII-region at the top of and two smaller HII-regions close to our candidate emission (red circles and clay circle in the left side of the first row in Figure 2). There are no known SNR candidates close to the candidate whereas in the large-field of Aur05 region of ~10° there are five known SNRs from the Green SNR catalog (SNR G166.0+04.3, SNR G166.3+02.5, etc., ~2 degree far away from the selected clay circle). The Sge01(A) (the right image on the third row in Figure 1) is a wide-field emission region including only one detected small (radius of 0.04°) HII-region defined in the WISE-HII catalog (red circle in the left side of the second row of Figure 2 with the clay circle for the emission field). Neither inside of the region nor close to the region there is no detected supernova remnant published under the Green 2019 catalog. In the region of our last emission candidate of Cep00(A) field (see the image in the fourth row in Figure 1) there are few HII-regions (red circles in the right image of the second row of Figure 2) with a smaller radius, are located both on the edge and outer side of the emission candidate (clay circle). There are detected SNRs very close to the field (ex. CTB 109 SNR) (green circles) and even the extension of the detected SNRs flow into the selected emission region. Currently, the main structure area still remains an unidentified type.

Finally, the standard identification technique for identifying the type of emission nebulae optically gives the flux ratio of [SII]/Hα $\geqslant$ 0.4. During this work, the reduction of the optical imaging data is done for only three out of seven nebulae (name of Cep00(A), Sge01(A), and Aur05(A)). For the reduction analysis of each candidate, the structures are divided into several regions; four regions over Cep00(A), two regions over both Sge01(A) and Aur05(A) (see the central coordinates of regions in Table 2). Each regions are shown with boxes of 21'.5 x 21'.5, same as of T100 field-of-view (FoV) (see the continuum-subtracted optical images of these regions, Aur05(A);Figure 3, Sge01(A);Figure 4 and Cep00(A);Figure 5). Since the identification technique applied to imaging for the three emission fields is satisfied the criterion [SII]/Hα $\geqslant$ 0.4, it becomes easier to mark these complicated emission fields as SNR candidates.

Table 2. Journal of T100 optical imaging observations for the three emission nebulae divided into several regions are shown with the boxes of size in 21'.5 x 21'.5 .The central coordinates of each region are shown with J2000 coordinates.

Regions Name	R.A. (J2000.0)	Dec. (J2000.0)
Cep00(A) region1	23:04:34.20	+58:20:33
Cep00(A) region2	23:03:49.89	+57:57:44
Cep00(A) region3	23:00:29.28	+57:39:43
Cep00(A) region4	23:02:26.38	+58:28:15
Sge01(A) region1	19:46:05.09	+17:56:17
Sge01(A) region2	20:02:50.49	+17:41:25
Aur05(A) region1	05:25:00.14	+40:08:18
Aur05(A) region2	05:29:51.82	+39:56:26

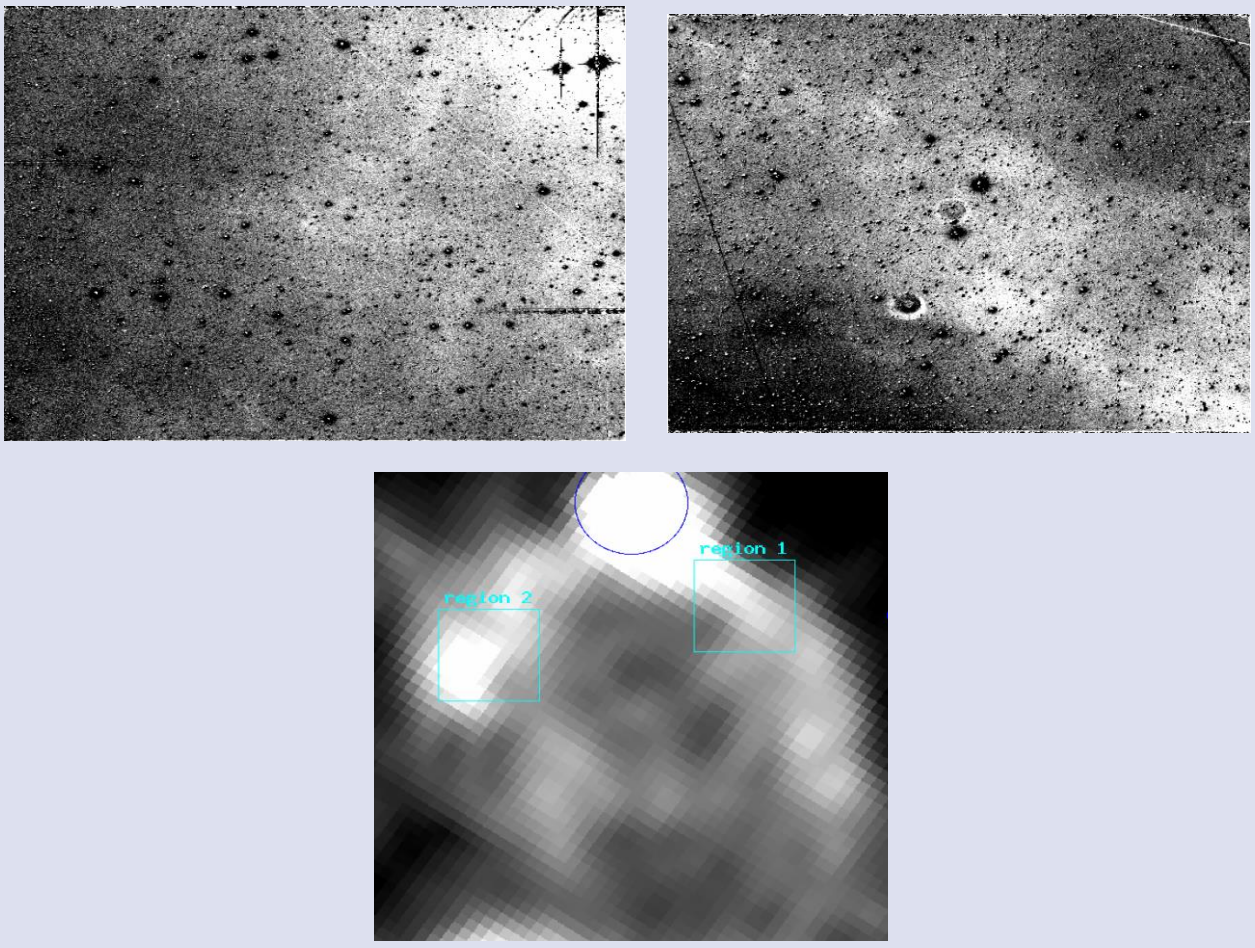

Figure 3. Hα image of the selected emission nebula in Aur05(A) field. North is up; east is to the left for the VTSS image. Approximate central coordinate of the 1.0°-structure is α(J2000) = 05h26m53s.0, δ(J2000) = +39° 41' 23". The two regions selected over the structure (detected HII-region shown with blue circle) are located in the Hα image. The continuum-subtracted images, observed with T100 observatory, used to determine the ratio of [SII]/Hα images are shown in the upper row, respectively, the image of region 2 (left side) and region 1 (right side).

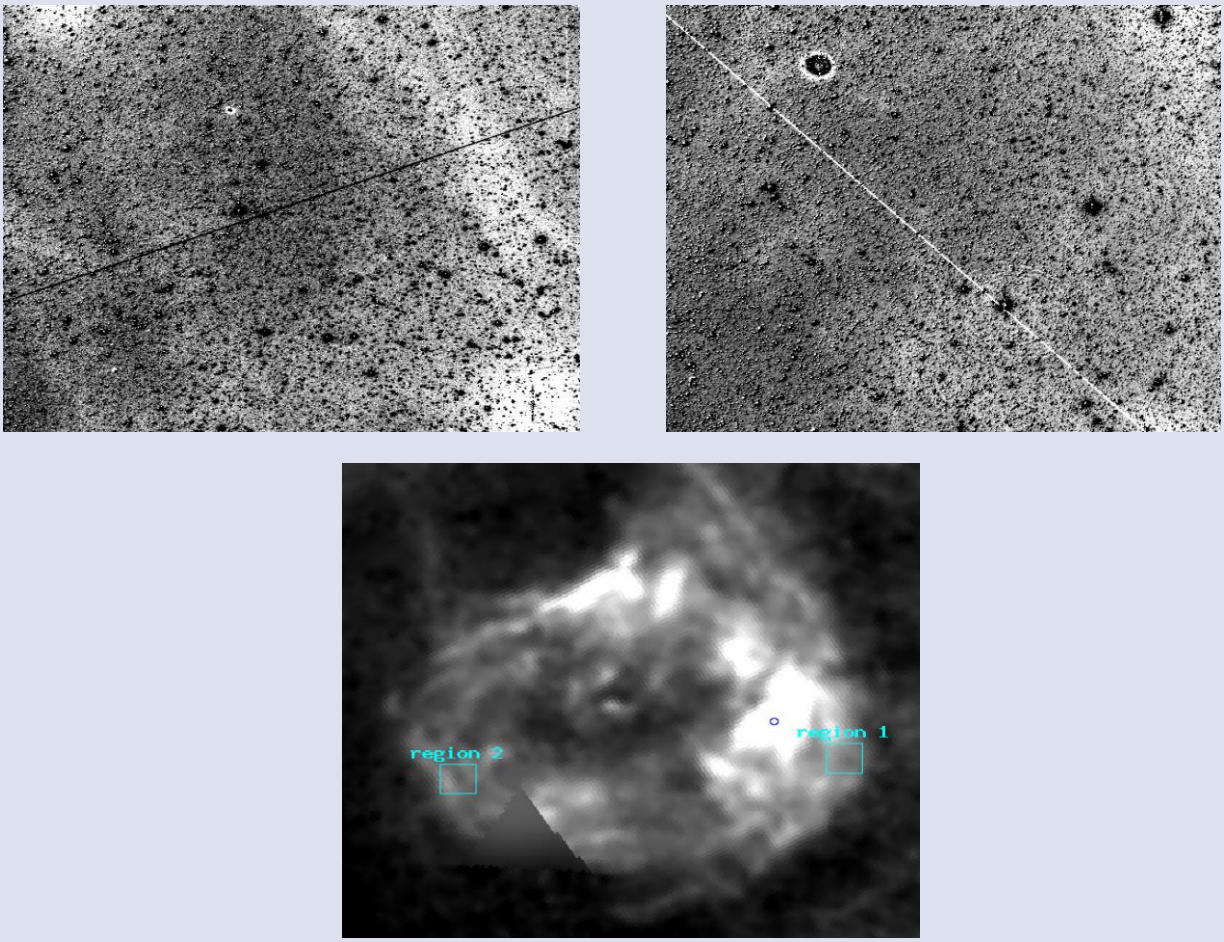

Figure 4. Hα VTSS image of emission nebula in Sge01(A) field. North is up; east is to the left for both VTSS survey image. Approximate central coordinate of the 2.5°-structure image is α(J2000) = 19h55m23s.0, δ(J2000) = +18° 37' 09''. The two regions selected over the structure (detected HII-region shown with blue circle) are located in the Hα image. The continuum-subtracted images, observed with T100 observatory, used to determine the ratio of [SII]/Hα images are shown in the upper row, respectively, the image of region 2 (left side) and region 1 (right side).

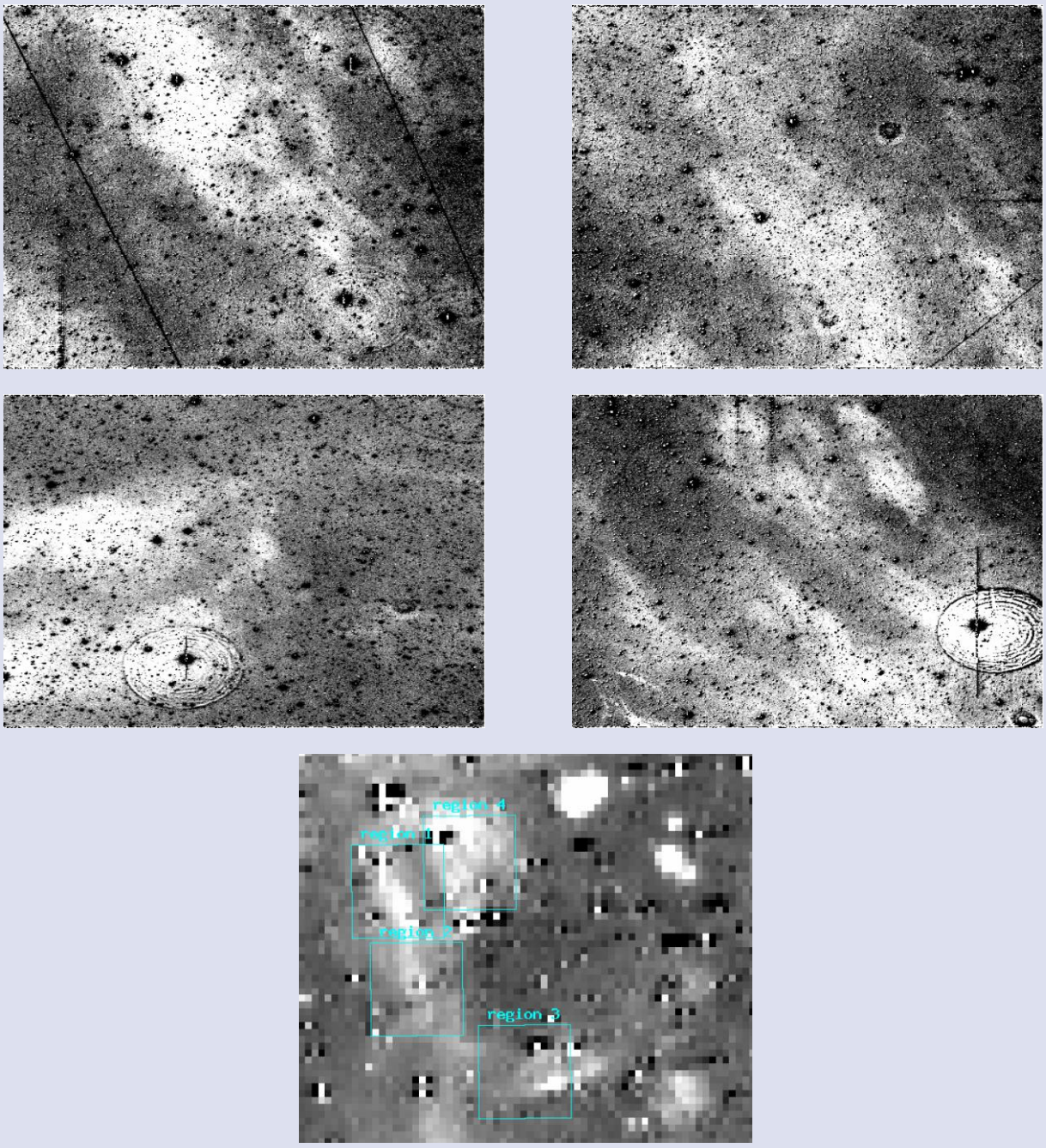

Figure 5. Hα VTSS image of emission nebula in Cep00(A) field. North is up; east is to the left for both the below VTSS survey image. Approximate central coordinate of the 1.0°-structure image is α(J2000) = 23h02m19s.0, δ(J2000) = +58° 07' 32". The four regions selected over the structure are located in the Hα image. The continuum-subtracted images, observed with T100 observatory, used to determine the ratio of [SII]/Hα images are shown in the upper two rows, respectively, the image of region 1 (upper left side), region 2 (upper right side), region 3 (middle left side) and region 4 (middle right side).

The identification technique results having values larger than 0.4 for the three of all give a possibility for the other four nebulae about being a strong SNR candidate even though we have no imaging information currently. These all candidates are in SNR- and HII-rich regions although there are no previously detected or identified emission structures within the specific areas around the given central coordinates, by using any known catalogs. This situation puts these candidates on top of the new observation list prepared for possible SNR candidates.

In future work, the missing optical imaging for some of the fields and the detailed optical spectroscopic of all fields should be completed. Besides the optical work, complementary search in the radio and X-ray will allow us to fully understand the physical properties of these supernova remnants with their contribution to the environment ISM and our own galaxy.

Acknowledgements

I would like to thank TÜBITAK National Observatory for a partial support in using T100 telescope with project number 18AT100-1309. Also, I would like to thank the Virginia Tech Spectral-Line Survey (VTSS), which is supported by the National Science Foundation. This work made use of Astropy (http://www.astropy.org) a community-developed core Python package and an ecosystem of tools and resources for astronomy [30,31]. I thank the referee for comments and a careful reading that helped to improve the clarity of the paper.

Conflicts of interest

There are no conflicts of interest in this work.

References

[1] Green D.A., A revised catalogue of 294 Galactic supernova remnants, *J. Astrophys. Astr.*, 40 (4) (2019) 36-48.

[2] Downes D., New Radio Results on Supernova Remnants, *AJ*, 76 (1971) 305-316.

[3] Chevalier R.A., The interaction of supernovae with the interstellar medium, *ARAA*, 15 (1977) 175-196.

[4] Kopsacheili M., Zezas A., Leonidaki I., A diagnostic tool for the identification of supernova remnants, *MNRAS*, 491 (2020) 889-902.

[5] Boumis P., Xilouris E. M., Alikakos J., Christopoulou,P. E., Mavromatakis F, Katsiyannis A. C., Goudis C. D., Discovery of optical emission from the supernova remnant G 32.8-0.1 (Kes 78), *A&A*, 499 (3) (2009) 789-797.

[6] Stupar, M., Parker Q. A., Optical detection and spectroscopic confirmation of supernova remnant G213.0-0.6 (now redesignated as G213.3-0.4), *MNRAS*, 419 (2) (2012) 1413-1420.

[7] Neustadt J. M. M., Fesen R. A., Black C. S., Detection of optical emission associated with the Galactic SNR G64.5+0.9, *MNRAS*, 469 (2017) 516-520.

[8] Stupar M., Parker Q. A., Frew D. J., Confirmation of G6.31+0.54 as a part of a Galactic supernova remnant, *MNRAS*, 479 (2018) 4432-4439.

[9] How T. G., Fesen R. A., Neustadt J. M. M., Black C. S., Outter, N., Optical emission associated with the Galactic supernova remnant G179.0+2.6, MNRAS, 478 (2) (2018) 1987-1993.

[10] Fesen R. A., Neustadt J. M. M., How T. G., Black C. S., Detection of extensive optical emission from the extremely radio faint Galactic supernova remnant G182.4+4.3, *MNRAS*, 486 (4) (2019) 4701- 4709.

[11] Fesen R.A., Weil K. E., Raymond J.C., Huet L., Rusterholz M., Di Cicco D., Mittelman D., Walker S., Drechsler M. and Faworski S., G107.0+9.0: a new large optically bright, radio, and X-Ray faint galactic supernova remnant in Cepheus, *MNRAS*, 498 (4) (2020) 5194–5206.

[12] Fesen R.A., Neustadt J.M.M., Black C.S. and Koeppel. A.H.D., Discovery of an Apparent High Latitude Galactic Supernova Remnant, *AJ*, 812 (1) (2015) 37-48.

[13] Stupar M., Parker Q. A., Filipovic M. D., Newly confirmed and candidate Galactic SNRs uncovered from the AAO/UKST Hα survey, *MNRAS*, 390 (3) (2008) 1037-1054.

[14] Fesen R. A., Milisavljevic D., Optical Discovery of an Apparent Galactic Supernova Remnant G159.6+7.3, *AJ*, 140 (5) (2010) 1163-1167.

[15] Sabin L., Parker Q. A., Contreras M. E., Olguín L., Frew D. J., Stupar M., Vázquez R., Wright N. J., Corradi R. L. M., Morris R. A. H., New Galactic supernova remnants discovered with IPHAS, *MNRAS*, 431 (1) (2013) 279-291.

[16] Dennison B., Simonetti J. H., Topasna G. A., An imaging survey of northern galactic Hα emmission with arcminute resolution, *PASA*, 15 (1) (1998) 147-148.

[17] Finkbeiner D.P., A Full-Sky Hα Template for Microwave Foreground Prediction, *ApJS*, 146 (2) (2003) 407-415.

[18] [Gaustad J. E., McCullough P. R., Rosing W., and Buren D. Van, A Robotic Wide-Angle Hα Survey of the Southern Sky, *PASP*, 113 (789) (2001) 1326–1348.

[19] Drew J.E., Greimel R., Irwin M.J., et al., The INT Photometric Hα Survey of the Northern Galactic Plane (IPHAS), *MNRAS*, 362 (3) (2005) 753-776.

[20] González-Solares E.A., Walton N.A, Greimel R., et al., Initial data release from the INT Photometric Hα Survey of the Northern Galactic Plane (IPHAS), *MNRAS*, 388 (1) (2008) 89-104.

[21] Mathewson, D. S., Clarke, J. N., Supernova Remnants in the Magellanic Clouds, *AJ*, 182 (1973) 697-698.

[22] Blair W. P., Kirshner R. P., Chevalier R. A., Supernova remants in M31, *ApJ*, 247 (1981) 879-893.

[23] Dopita M.A., Benvenuti P., Dodorico S., Binette L., Radiative shock-wave theory. I. Chemical abundance diagnostics and galactic abundance gradients, *ApJ*, 276 (1984) 653-666.

[24] Fesen R. A., Blair W. P., Kirshner R. P., Optical emission-line properties of evolved galactic supernova remnants, *AJ*, 292 (1985) 29-48.

[25] Leonidaki I., Boumis P., Zezas A., A multiwavelength study of supernova remnants in six nearby galaxies - II. New optically selected supernova remnants, *MNRAS*, 429 (1) (2013) 189-220.

[26] Long K. S., Galactic and Extragalactic Samples of Supernova Remnants: How They Are Identified and What They Tell Us, in Alsabti A. W., Murdin P., eds, Handbook of Supernovae, *Springer International Publishing AG*, (2017) 2005-2040.

[27] https://doi.org/10.1007/978-3-319-21846-5_90

[28] Frew D.J., Bojicic I.S., Parker Q.A., A catalogue of integrated Hα fluxes for 1258 Galactic planetary nebulae, *MNRAS*, 431 (1) (2013) 2–26.

[29] Dharmawardena T. E., Barlow M. J., Drew J. E., Seales A., Sale S. E., Jones D., Mampaso A., Parker Q. A., Sabin L., Wesson R., Hα fluxes and extinction distances for planetary nebulae in the IPHAS survey of the northern galactic plane, *MNRAS*, 501 (4) (2021) 6156–6167.

[30] Anderson L.D., Bania T.M., Balser D. S., Cunningham V., Wenger T. V., Johnstone B.M., and Armentrout W.P., The WISE Catalog of Galactic H II Regions, *ApJS*, 212 (1) (2014) 1–18.

[31] The Astropy Collaboration, Astropy: A community-developed core Python package and an ecosystem of tools and resources for astronomy, *AA*, 558 (2013) A33.

[32] The Astropy Collaboration, Astropy: A community-developed core Python package and an ecosystem of tools and resources for astronomy, *AJ*, 156 (2018) 123.